NATIONAL ADVISORY COMMITTEE FOR AERONAUTICS

REPORT No. 608

STRESS ANALYSIS OF BEAMS WITH SHEAR DEFORMATION OF THE FLANGES

By PAUL KUHN

1937

For sale by the Superintendent of Documents, Washington, D. C.
Subscription price, $5 per year

AERONAUTIC SYMBOLS

1. FUNDAMENTAL AND DERIVED UNITS

	Symbol	Metric		English	
		Unit	Abbreviation	Unit	Abbreviation
Length	l	meter	m	foot (or mile)	ft. (or mi.)
Time	t	second	s	second (or hour)	sec. (or hr.)
Force	F	weight of 1 kilogram	kg	weight of 1 pound	lb.
Power	P	horsepower (metric)		horsepower	hp.
Speed	V	kilometers per hour	k.p.h.	miles per hour	m.p.h.
		meters per second	m.p.s.	feet per second	f.p.s.

2. GENERAL SYMBOLS

W, Weight$=mg$

g, Standard acceleration of gravity$=9.80665$ m/s^2 or 32.1740 ft./sec.^{2}

m, Mass$=\frac{W}{g}$

I, Moment of inertia$=mk^2$. (Indicate axis of radius of gyration k by proper subscript.)

μ, Coefficient of viscosity

ν, Kinematic viscosity

ρ, Density (mass per unit volume)

Standard density of dry air, 0.12497 kg-m^{-4}-s^2 at 15° C. and 760 mm; or 0.002378 lb.-ft.$^{-4}$ sec.^{2}

Specific weight of "standard" air, 1.2255 kg/m^3 or 0.07651 lb./cu. ft.

3. AERODYNAMIC SYMBOLS

S, Area

S_w, Area of wing

G, Gap

b, Span

c, Chord

$\frac{b^2}{S}$, Aspect ratio

V, True air speed

q, Dynamic pressure$=\frac{1}{2}\rho V^2$

L, Lift, absolute coefficient $C_L=\frac{L}{qS}$

D, Drag, absolute coefficient $C_D=\frac{D}{qS}$

D_0, Profile drag, absolute coefficient $C_{D_0}=\frac{D_0}{qS}$

D_i, Induced drag, absolute coefficient $C_{D_i}=\frac{D_i}{qS}$

D_p, Parasite drag, absolute coefficient $C_{D_p}=\frac{D_p}{qS}$

C, Cross-wind force, absolute coefficient $C_C=\frac{C}{qS}$

R, Resultant force

i_w, Angle of setting of wings (relative to thrust line)

i_t, Angle of stabilizer setting (relative to thrust line)

Q, Resultant moment

Ω, Resultant angular velocity

$\rho\frac{Vl}{\mu}$, Reynolds Number, where l is a linear dimension (e.g., for a model airfoil 3 in. chord, 100 m.p.h. normal pressure at 15° C., the corresponding number is 234,000; or for a model of 10 cm chord, 40 m.p.s., the corresponding number is 274,000)

C_p, Center-of-pressure coefficient (ratio of distance of c.p. from leading edge to chord length)

α, Angle of attack

ϵ, Angle of downwash

α_0, Angle of attack, infinite aspect ratio

α_i, Angle of attack, induced

α_a, Angle of attack, absolute (measured from zero-lift position)

γ, Flight-path angle

REPORT No. 608

STRESS ANALYSIS OF BEAMS WITH SHEAR DEFORMATION OF THE FLANGES

By PAUL KUHN

Langley Memorial Aeronautical Laboratory

NATIONAL ADVISORY COMMITTEE FOR AERONAUTICS

HEADQUARTERS, NAVY BUILDING, WASHINGTON, D. C.

LABORATORIES, LANGLEY FIELD, VA.

Created by act of Congress approved March 3, 1915, for the supervision and direction of the scientific study of the problems of flight (U. S. Code, Title 50, Sec. 151). Its membership was increased to 15 by act approved March 2, 1929. The members are appointed by the President, and serve as such without compensation.

TECHNICAL COMMITTEES

AERODYNAMICS
POWER PLANTS FOR AIRCRAFT
AIRCRAFT MATERIALS
AIRCRAFT STRUCTURES
AIRCRAFT ACCIDENTS
INVENTIONS AND DESIGNS

Coordination of Research Needs of Military and Civil Aviation

Preparation of Research Programs

Allocation of Problems

Prevention of Duplication

Consideration of Inventions

LANGLEY MEMORIAL AERONAUTICAL LABORATORY

LANGLEY FIELD, VA.

Unified conduct, for all agencies, of scientific research on the fundamental problems of flight.

OFFICE OF AERONAUTICAL INTELLIGENCE

WASHINGTON, D. C.

Collection, classification, compilation, and dissemination of scientific and technical information on aeronautics.

REPORT No. 608

STRESS ANALYSIS OF BEAMS WITH SHEAR DEFORMATION OF THE FLANGES

By PAUL KUHN

SUMMARY

The fundamental action of shear deformation of the flanges is discussed on the basis of simplifying assumptions. The theory is developed to the point of giving analytical solutions for simple cases of beams and of skin-stringer panels under axial load. Strain-gage tests on a tension panel and on a beam corresponding to these simple cases are described and the results are compared with analytical results. For wing beams, an approximate method of applying the theory is given. As an alternative, the construction of a mechanical analyzer is advocated.

INTRODUCTION

The so-called "semimonocoque" type of construction, which has been favored by aircraft designers for some time, presents serious difficulties in stress analysis. Static tests have proved that the bending action of such a structure is not always described with sufficient accuracy by the standard engineering formulas based on the assumption that plane cross sections remain plane. It will be necessary, therefore, to devise new working theories for the action of semimonocoque beams under bending loads.

In order to arrive at reasonably rapid methods of stress analysis, it is necessary to make rather sweeping assumptions. It is obvious that the range of applicability of any such method is limited. The present paper concerns itself with beams typical in general form of one class of beams used in airplane construction, that is, with *fairly shallow, wide beams, having flat covers, symmetrical about the center line, with two shear webs and with bulkheads that offer no appreciable resistance to deformation out of their planes.*

Briefly, the action of such a beam under loads applied at the shear webs is as follows: The transverse shear is taken up by the shear webs. The flanges attached to these shear webs furnish part of the longitudinal stresses required to balance the external bending moment. The strains set up by these stresses induce shear stresses in the skin which, in turn, cause longitudinal stresses in the intermediate stringers attached to the skin until sufficient longitudinal stresses exist at any section to balance the external bending moment.

If the skin between stringers did not deform under the action of the shear stresses, the standard beam formulas would apply. The thin sheet, however, has very little shear stiffness and suffers large deformations under load. As a result, the first intermediate stringer next to a shear web carries a smaller stress than the flange of the shear web, the next intermediate stringer carries less stress than the first one, and so on to the center stringer, which carries the smallest stress. This phenomenon of the interdependence between stringer stresses and shear deformations forms the subject of the present paper.

Apparently Dr. Younger was the first person in this country to give serious attention to this subject. In reference 1 he gives a formula for the efficiency of a box beam with walls of uniform thickness, which may be considered as the limiting case of very many extremely small stringers. Nothing more on the subject was published until two experimental studies appeared in 1936. Reference 2, dealing with the case of a skin-stringer panel in edge compression, includes a theoretical solution for a particular case. Reference 3 deals with a box beam in pure bending, a problem identical with the one treated in reference 2. In both studies the stringer stresses experimentally obtained were used to compute efficiency factors for the shear stiffness of the sheet.

The most important practical problem is the inverse of the problem dealt with in references 2 and 3; namely, given the shear stiffness, to calculate the stringer stresses. The problem is difficult and complex. In order to arrive at any solution, it has been necessary to use a very much simplified concept of the action of the structure, as suggested in references 1 and 2. On the basis of this simplified concept, the analytical solutions for a few very simple cases of axially loaded panels and of beams are derived in this paper. For other cases, it will be shown that a trial-and-error method of solution is feasible.

The analytical solutions as well as the trial-and-error method apply only to very elementary cases, namely, to three-stringer panels under axial load and to beams with a single longitudinal stringer attached at the center line of the cover sheet. It has been considered worth while to devote considerable space to the discussion of these elementary cases for the following reasons:

1. The study of these simple cases greatly facilitates the understanding of the fundamental principles. (It is very strongly urged that anyone desiring to use the

The condition of a pure diagonal-tension field is not reached, however, until the buckling shear stress has been considerably exceeded. Consequently, values intermediate between G and $\frac{5}{8}G$ will occur at stresses not too greatly in excess of the buckling stress (i. e., 3 to 5 times), provided that the edge members are sufficiently stiff. If the edge members are not sufficiently stiff or well braced to take the transverse component of the diagonal tension and particularly if the sheet carries edge compression in addition to shear, the shear stiffness may drop to very low values. Values as low as $G_e = 0.1G$ have been reported (reference 3); although the numerical accuracy of this particular analysis has been questioned, it serves at least as a useful indication of what may be expected, remembering that this test was stopped long before reaching the ultimate load. Quantitative information on this subject is scarce. Fortunately, as will be shown later, the shear stiffness need not be very accurately known to obtain reasonable accuracy in the stringer stresses.

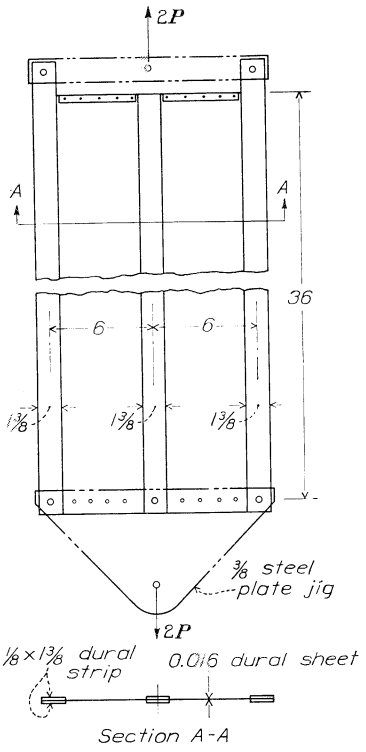

FIGURE 5.—Test panel.

It is clear that the sheet will not only act as a shear member in accordance with the theory but will also assist in carrying longitudinal stresses. The following assumptions have been used:

1. For a sheet carrying tension in addition to shear, it was assumed that the sheet is fully effective in tension; i. e., the sheet up to a line halfway between the stringers is added to the stringer proper when computing the cross-sectional area of the stringer. This assumption is obviously somewhat unsafe and should be modified when the stringer stresses are high.

2. For a sheet carrying compression in addition to the shear, von Kármán's formula for effective width was used in the form

$$2w = 1.9\sqrt{\frac{E}{\sigma}}t$$

where w is the effective width (on one side of the stringer) and σ the stress in the stringer. This formula is probably always conservative in the range in question.

COMPARISON BETWEEN TEST AND CALCULATED RESULTS

In order to check the validity of the method thus far developed, a test specimen was built to represent a structure corresponding to figure 1 (a). A sketch of the actual test specimen is shown in figure 5. Pin-end steel bars (not shown in the figure) spaced 3 inches apart were used to separate the edge stringers from the central stringer and to take up the transverse component of the diagonal-tension field that developed under load. In each bay between these bars, the strains in the stringers were measured with 2-inch Tuckerman strain gages on both sides of the specimen. This precaution proved necessary because the stresses on the two sides differed so much at some stations that readings on only one side would have been almost useless.

The load was increased from zero to the maximum of 4,800 pounds in five steps. With a very few minor exceptions, the points for any one gage fell on straight lines. For each station, the results obtained on the front and the back of the specimen were averaged and the average values are plotted in figure 6.

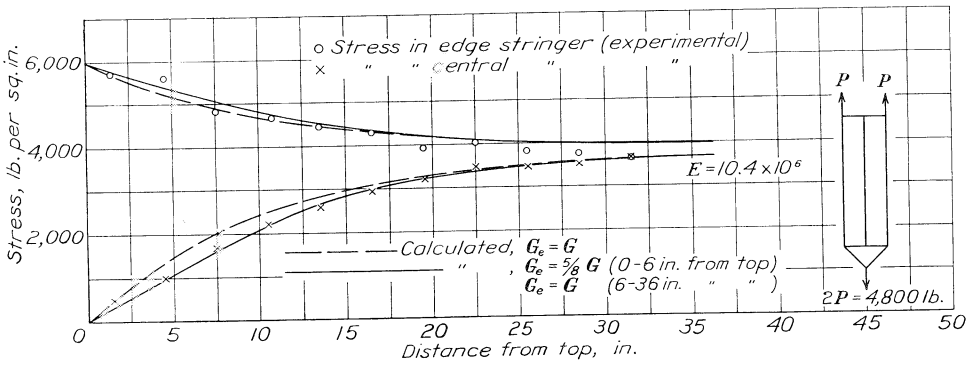

FIGURE 6.—Comparisons between calculated and experimental results for tension test panel.

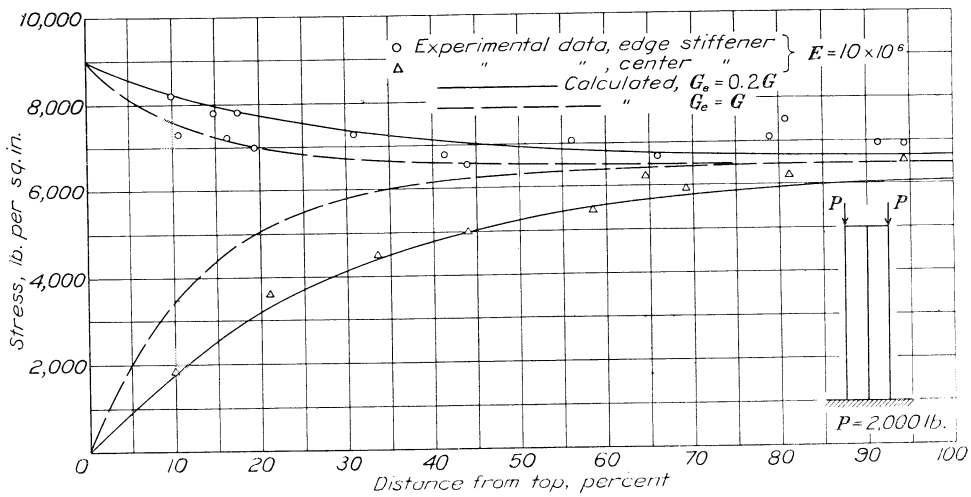

FIGURE 7.—Comparison between calculated and experimental results for compression test panel. (Data from reference 2.)

The calculations were made for the two different assumptions of the shear stiffness indicated on the figure. The second assumption of $G_e = \frac{5}{8}G$ in the top part was based on the experimentally observed fact that one well-developed diagonal-tension fold showed in the top of the panel on each side, in agreement with the calculation showing that at the maximum load the shear stress in this region was about six times the buckling stress.

The second assumption gives perfect agreement between calculated and test results for the stress in the central stringer. The agreement is not quite so good on the edge stringer, the discrepancy occurring chiefly at the root. Several explanations of the discrepancy may be offered. An error of several percent may be caused by an error in the value of E assumed to convert strain readings to stress readings. The simple theory used may break down to some extent near the root and, finally, jig deflection may cause errors. The steel triangle used on the lower end is not a rigid foundation, and a slight elastic deformation of this steel triangle under the edge stringers would relieve the edge stringers of some load and throw it into the sheet and possibly into the central stringer. A deformation of about 0.0003 inch would be sufficient to make the calculated stringer stresses equal at the jig end. Undoubtedly the assumptions of effective areas, effective shear stiffness, and jig deflection could be varied within their possible limits to give a much better agreement with the experimental points.

A similar analysis was made for the panel tested in compression as described in reference 2. The results are shown in figure 7. It will be noted that fair agreement with the experimental points is obtained by assuming that the effective shear stiffness is only 0.2 the shear modulus, in marked contrast to the tension panel. The curves calculated with $G_e = G$ are also given to show the extent to which possible variations in G_e affect the stringer stresses.

BEAMS WITH ONE LONGITUDINAL

BEAM OF CONSTANT DEPTH

The simplest case of a beam subjected to shear deformation of the flange is shown in figure 8. For simplicity of the sketch the flange material on the side not under consideration is assumed to be concentrated at the shear web. This assumption does not influence the analysis when the cover is flat.

For convenience of discussion, the material concentrated at the top of the shear web will be referred to as the "flange" throughout this paper, while the stringer attached to the cover sheet will be referred to as the "longitudinal."

It is again assumed that the longitudinal is cut along the line of symmetry (fig. 8 (b)). The force acting on this halved longitudinal is denoted by F_L, the force on the (tension) flange by F_F. The shear force in the web

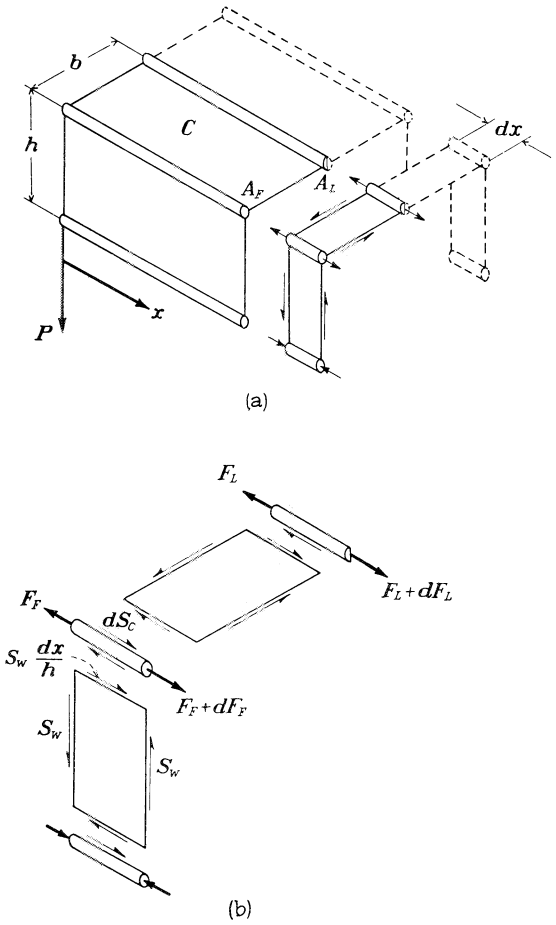

FIGURE 8.—Beam with flat cover and one longitudinal.

is denoted by S_W; the shear force in the cover sheet, by S_C.

The governing equations are

$$dF_F = S_W \frac{dx}{h} - dS_C \tag{3a}$$

$$-dF_L = dS_C \tag{3b}$$

$$d\tau = -\frac{G_e}{Eb}(\sigma_F - \sigma_L)\, dx \tag{3c}$$

with the auxiliary equations

$$\sigma_F = \frac{F_F}{A_F};\ \sigma_L = \frac{F_L}{A_L};\ S_W = P;\ dS_C = \tau t dx$$

The solution of the resulting differential equation is given in appendix B, Case 3 (*a*).

COMPARISON BETWEEN TEST AND CALCULATED RESULTS

The test panel that had been used in the previously described tension test was slightly modified and attached to two duralumin I-beams to form an open

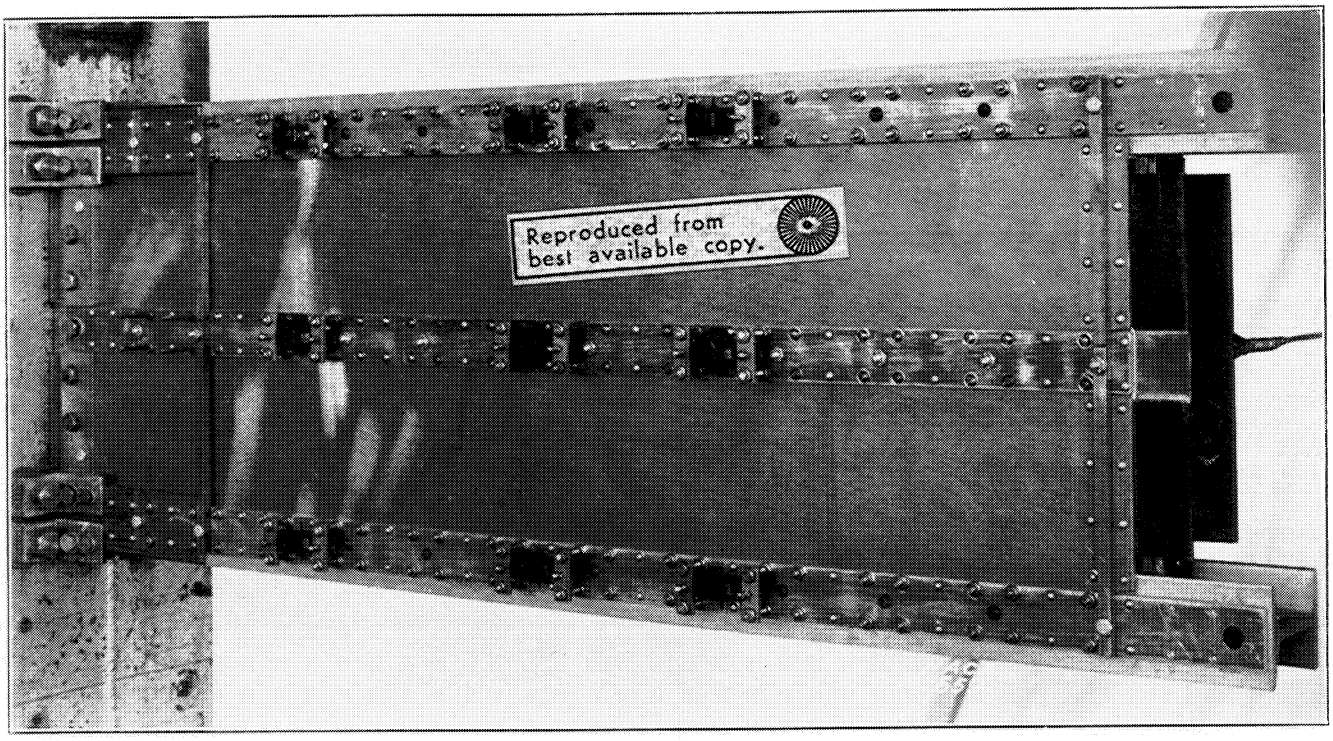

(a) Closed side.

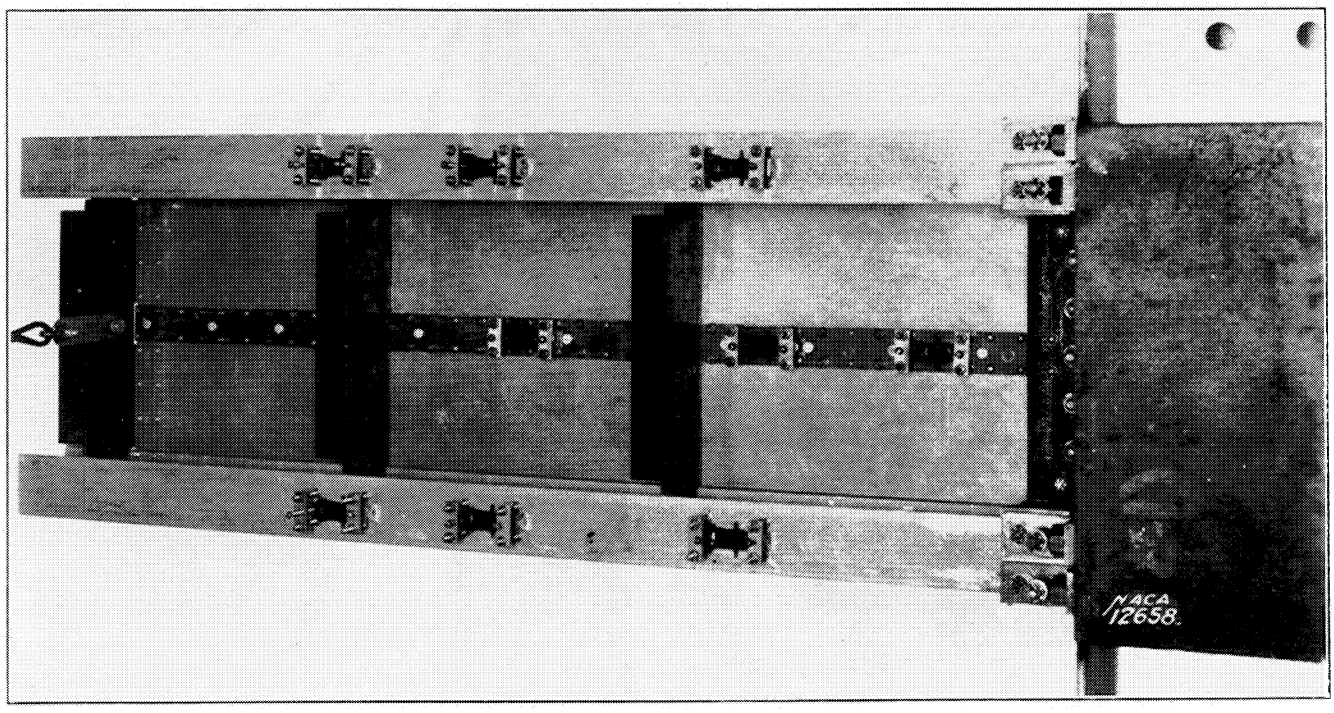

(b) Open side.

FIGURE 9.—View of test beam, showing strain gages.

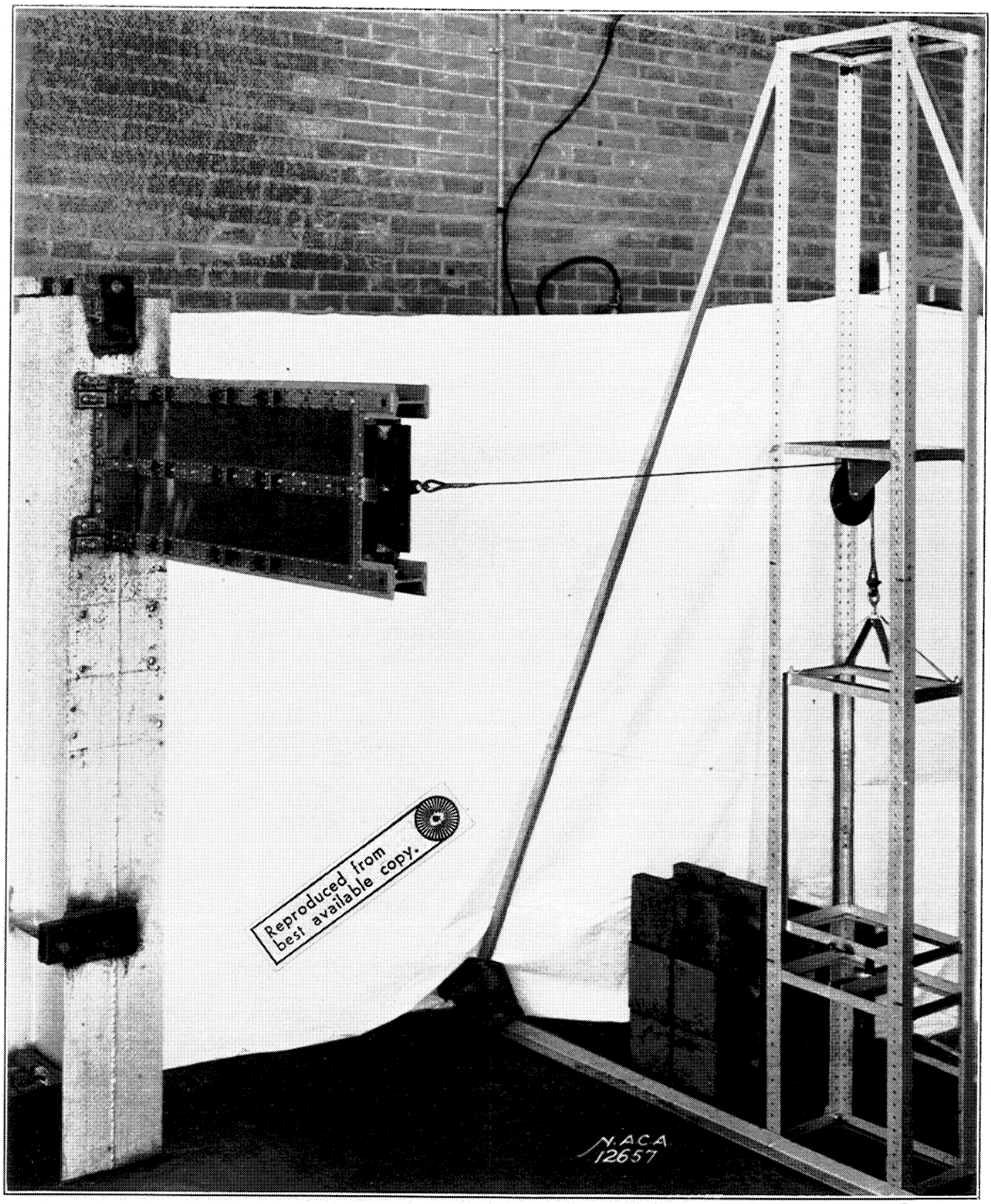

FIGURE 10.—Set-up for testing beams.

box beam. Figure 9 shows photographs of the beam with the strain gages in place for a test run; figure 10 shows the test set-up. The cross section of this beam is shown in figure 11.

It should be noted that the cover sheet and the longitudinal were not attached to the bulkheads except at the root. The flange material of the I-beams (including the cover strips riveted to them and the sheet material effective in tension) was replaced, for the purpose of analysis, by equivalent concentrated flanges with a centroidal distance of 2.80 inches (effective depth h of beam, fig. 8 (a)). The calculated stresses are therefore valid for the flange centroids. For comparison with the measured stresses, the calculated flange stresses were corrected to the outside fiber stresses

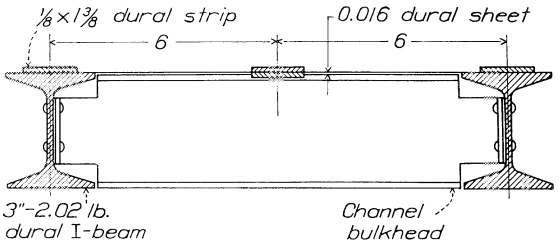

FIGURE 11.—Cross section on test beam.

under the assumption that plane cross sections remain plane for the I-beams with cover strips.

Figure 12 shows the experimental points, the curves calculated for three different assumptions of the shear stiffness, and the stresses calculated by the ordinary bending theory. It can be seen that the experimental points group fairly well about the curve for $G_e = \frac{5}{8}\ G$, particularly when this curve is corrected for an estimated jig deflection by the formula in appendix B, case 2. Close to the root, however, discrepancies are again observed as in the case of the tension panel. The high flange stress at the station nearest the root may perhaps be explained by nonlinear stress distribution in the I-beams caused by the method of attaching them to the jig, which was not designed for this test. The reduction in shear stiffness of the sheet as compared with the stiffness developed by the same sheet in the tension panel can be ascribed to numerous initial buckles present in the beam but not in the tension panel.

Inspection of figure 12 shows that very large variations of shear stiffness have only a relatively small influence on the bending stresses. This result is due to the fact that, even when the shear stiffness increases to infinity, the bending stresses never exceed a finite limiting value. In many actual structures, the shear stiffness provided is sufficiently large to permit the limiting stress to be approached within a few percent. Practically speaking, this fact means that the shear stiffness need not be very accurately known to obtain the necessary accuracy in the bending stresses.

BEAM OF VARIABLE DEPTH

In a beam with variable depth, the only change in the equations is introduced by the fact that the vertical components of the flange forces balance part of the applied shear, so that the shear in the web now becomes

$$S_W = S_a - \frac{M}{h}\ (\tan\ \beta + \tan\ \gamma) \qquad (5)$$

where β and γ are the angles of inclination of the tension flange and of the compression flange.

The analytical solution for a special case of a beam with variable depth is given in appendix B as Case 3 (b).

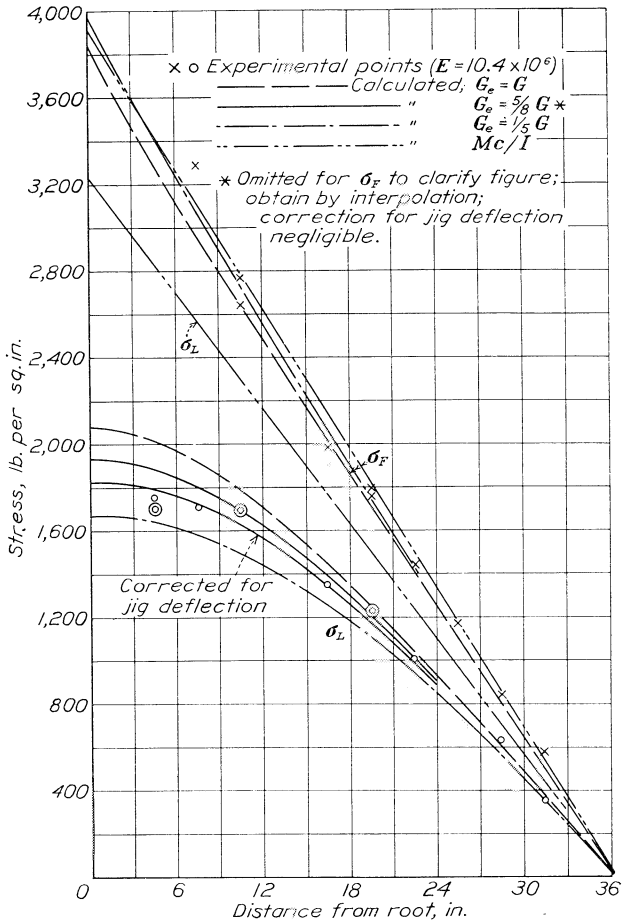

FIGURE 12.—Comparison between calculated and experimental results for test beam.

CONSTANT-STRESS SOLUTION FOR BEAMS WITH ONE LONGITUDINAL

The analytical solutions presented thus far, together with the trial-and-error method, are reasonably adequate for dealing with beams having one longitudinal. There appears to be but slight possibility, however, of extending these solutions to the practical cases of beams with a number of longitudinals. An approximate method will now be developed that can be extended to such beams. The method will first be developed for a beam with a single longitudinal because comparisons can be made with the exact solution to gain some idea of the reliability of the approximate method.

The approximate method is based on the following reasoning. It is the aim of the designer to dimension the structure so that the stress in it is uniform for the given loading. For several reasons this ideal is never reached, but there is usually an effort made to taper the dimensions so as to approach the dimensions of the ideal design. Now the solution for constant stress along the span can be very easily obtained. It is possible, therefore, to consider the actual condition as a superposition upon the ideal case, which can be calculated exactly, of some additional disturbing cases or "faults." These faults can be calculated only approximately, but if they are of minor importance compared with the ideal case, the resulting error of the total solution will be small.

The detailed development of the method is as follows: The fundamental equation

$$d\tau=\frac{G_e}{Eb}(\sigma_F-\sigma_L)dx \tag{6}$$

can be integrated once, if σ_F and σ_L are constant as assumed, to give

$$\tau_x=\frac{(\sigma_F-\sigma_L)}{Eb}\int_0^x G_e dx=\frac{(\sigma_F-\sigma_L)x\overline{G}_x}{Eb} \tag{7}$$

where $\overline{G}_x$ is the shear stiffness averaged over the distance $x=0$ to $x=x$, and the x origin is taken at the root. Integrated again to give the total shear force in the cover sheet

$$S_C=\int_0^L \tau_x t dx=K_1(\sigma_F-\sigma_L) \tag{8}$$

For example, if G_e and t are constant along the span,

$$K_1=\frac{G_e t L^2}{2Eb}$$

Equation (8) furnishes one relation between σ_F and σ_L. One more relation is needed to complete the solution. There are infinitely many conditions from which to choose this relation. At any station along the span, the internal bending moment should equal the external bending moment. The root section has been chosen because in a number of trials it always proved, by far, to be the best choice. Equating the internal and external moment (applied at the root) gives the relation

$$(\sigma_F A_{F_0}+\sigma_L A_{L_0})h_0=M_{a_0} \tag{9}$$

Now remembering that

$$S_C=\sigma_L A_{L_0}$$

equations (8) and (9) can be solved for the bending stresses

$$\sigma_L=\frac{M_0 K_1}{h_0[A_{F_0}A_{L_0}+K_1(A_{F_0}+A_{L_0})]} \tag{10a}$$

$$\sigma_F=\frac{M_0(A_{L_0}+K_1)}{h_0[A_{F_0}A_{L_0}+K_1(A_{F_0}+A_{L_0})]} \tag{10b}$$

Substituting equations (10a) and (10b) into equation (7) gives

$$\tau=\frac{x\overline{G}_x M_0}{Ebh_0\left[A_{F_0}+K_1\left(1+\frac{A_{F_0}}{A_{L_0}}\right)\right]} \tag{10c}$$

Equations (10a), (10b), and (10c) constitute the "pure constant-stress solution" for a beam with a single longitudinal.

The internal bending moment at any station along the span can now be calculated

$$M_{int}=(\sigma_F A_F+\sigma_L A_L)h$$

and, in general, this internal moment will not be equal to the applied moment M_a. This difference constitutes the first fault of the constant-stress solution and will be called the "moment fault."

In order to remove this fault, additional (corrective) bending moments must be added, which are at any station

$$M'=M_a-M_{int}$$

the prime denoting corrective moments. The stresses caused by these corrective moments must be computed and added to the stresses of the pure constant-stress solution.

The method of computing the stresses caused by the corrective moments will be approximate and arbitrary as thus far no exact solutions of this problem have been found. The following method was chosen because the underlying assumption is the most obvious one and because the method is very convenient, eliminating the necessity of computing the internal moments, the corrective moments, and the corrective stresses separately.

From equations (10a) and (10b) it follows that the ratio

$$\left(\frac{\sigma_F}{\sigma_L}\right)_0=r_0=\left(1+\frac{A_{L_0}}{K_1}\right) \tag{11}$$

The assumption is now made that this ratio remains constant ($r=r_0$) along the span and that it holds not only for the stresses caused by the "ideal" moments but also for the stresses caused by the corrective moments. Under this assumption, the direct stresses at any station are given by

$$\sigma_F=\frac{M_a}{hA_F\left(1+\frac{A_L}{rA_F}\right)} \tag{12a}$$

$$\sigma_L=\frac{M_a}{hA_L\left(1+\frac{rA_F}{A_L}\right)} \tag{12b}$$

From these stresses the shear stresses are obtained by using the fundamental relation (2) and integrating from the root toward the tip

$$\tau=\int_0^x \frac{G_e}{Eb}(\sigma_F-\sigma_L)dx \tag{12c}$$

The moment fault has now been removed; that is, the internal moments equal the applied moments when the stresses as given by equations (12a) and (12b) exist in

The increments of corrective shear force are obtained by using equations (13), (14), and (15). After the integration of (15) in from the tip to obtain the corrective shear force S_C', the correction to the flange stress is calculated by the first expression of (16); the correction to the shear stress is calculated by the last expression of (16).

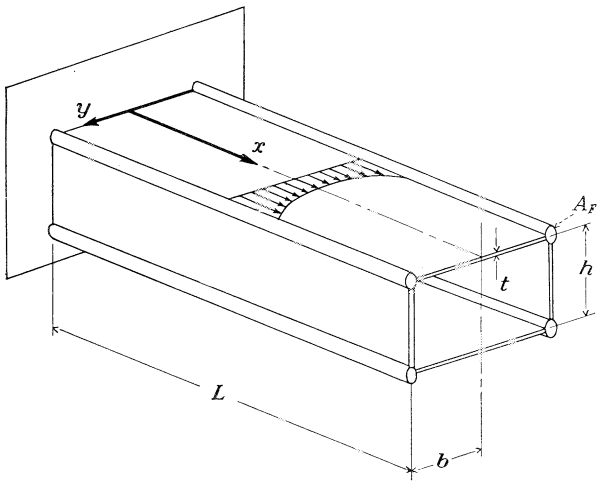

FIGURE 17.—Notation used for beams with orthotropic cover plates.

The calculation of the correction to the stress σ_L is somewhat more complicated because it varies along the chord. The total force on all longitudinals, using equation (17), is given by

$$F_L=\int_0^b \sigma\frac{A_L}{b}dy=\frac{A_L}{K_3b}\sigma_{CL}\sinh K_3b \tag{19}$$

where σ_{CL} denotes the stress at the center line of the beam obtained from equation (17) by setting $y=0$. In accordance with (16), only a part of the corrective shear force is applied so that the corrected total force on the longitudinals is

$$F_{L_{corr}}=F_L-C_1S_C' \tag{20}$$

Assume now that the corrected stresses in the longitudinals are distributed chordwise according to the law

$$\sigma_{corr}=\sigma_{CL_{corr}}\cosh Yy \tag{21}$$

The unknown Y can be found from the equation

$$\frac{\tanh Yb}{Yb}=\frac{F_{L_{corr}}}{A_L\sigma_{F_{corr}}} \tag{22}$$

which is based on the premise that

$$\sigma_{L_{corr}}=\sigma_{F_{corr}}$$

for $y=b$. After Y has been found, the corrected stress at the center line is found from

$$\sigma_{CL_{corr}}=\sigma_{F_{corr}}\operatorname{sech} Yb$$

and equation (21) can then be used to calculate the stresses at intermediate values of y. The right-hand side of equation (22) is the ratio of the average stress in the longitudinals to the stress in the flange. In general, this ratio will be less than unity; however, figure 16 shows that for a beam with a single longitudinal the stress in the longitudinal may be larger than the stress in the flange over a part of the span, and similarly the right-hand side of equation (22) sometimes may exceed unity. In such a case, equations (21) and (22) may be replaced by

$$\sigma_{corr}=\sigma_{CL_{corr}}(2-\cosh Yy) \tag{21a}$$

$$\frac{\left(2-\frac{\sinh Yb}{Yb}\right)}{(2-\cosh Yb)}=\frac{F_{L_{corr}}}{A_L\sigma_{F_{corr}}} \tag{22a}$$

After Y has been found, the corrected stress at the center line is found from

$$\sigma_{CL_{corr}}=\frac{\sigma_{F_{corr}}}{(2-\cosh Yb)}$$

and equation (21a) can then be used to calculate the stresses at intermediate values of y.

The solution of equations (22) and (22a) can be effected by inspection of tables. For practical purposes it should be sufficient to use the curve given on figure 18.

As examples, beams A and B were analyzed under the assumption that longitudinals with the total cross-sectional area A_L are distributed uniformly along the chord. The results are shown in figures 19 and 20. It will be seen that the stress at the center line of the beam is very low. If all longitudinals are of the same cross section, they must be designed to the stress in the first longitudinal adjacent to the flange. Consequently,

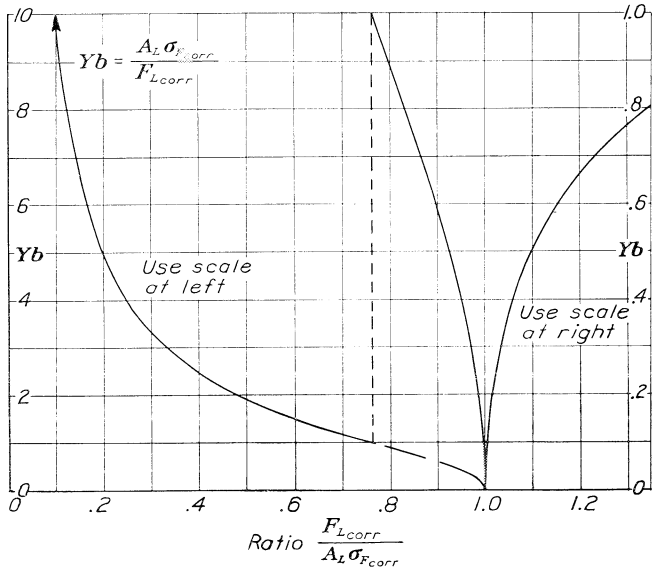

FIGURE 18.—Graph for auxiliary parameter Yb.

the longitudinals near the center line are very ineffectively used. In this connection, attention might be called to the fact that the longitudinals need not be of the same cross-sectional area along the chord. The

assumption of A_L being uniformly distributed may be fulfilled, for instance, by using longitudinals of large cross-sectional area but widely spaced near the flange and longitudinals of small cross-sectional area but closely spaced near the center line. Although such an arrangement would not increase the over-all structural efficiency, it might under certain conditions offer manufacturing advantages.

MECHANICAL ANALYZER

The constant-stress solution is always approximate. When the moment and shear corrections are large, doubts may arise as to whether the solution is sufficiently accurate. It might be advantageous to construct a mechanical analyzer to deal with such cases. One possibility for such an analyzer would be actually to build units representing the mechanical model sketched in figure 1 (b). The springs might be cantilever springs, so that their stiffnesses could be varied by changing their lengths. Each unit would represent one bay of the trial-and-error method of solution and would have one spring to represent the stringer stiffness and one spring to represent the shear stiffness of the sheet attached to one side of the stiffener.

The chief difficulty in the design of such an analyzer would probably be in reducing the friction between the units and the guides necessary to aline them. A fairly large number of units would be necessary to represent a wing cover, which would mean a fairly expensive instrument. This disadvantage is counterbalanced by

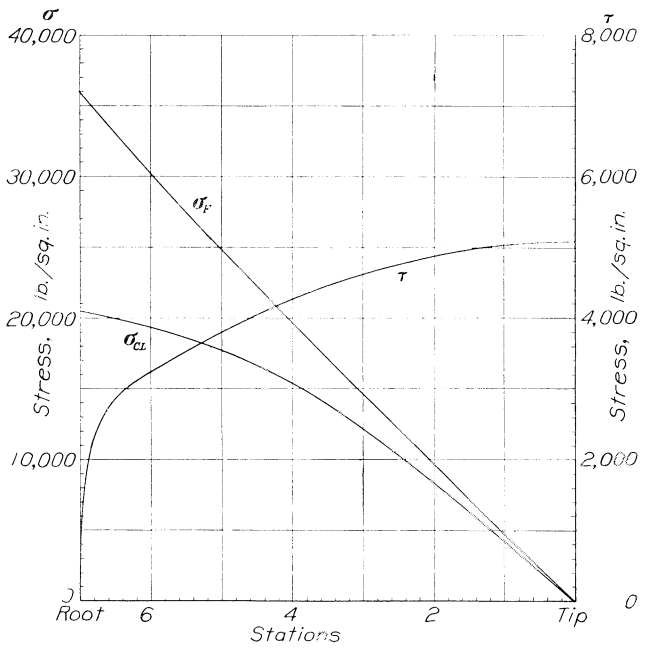

FIGURE 19.—Stresses in beam A with A_L uniformly distributed along chord.

the possibility that the instrument would offer in a comparatively short time quite an exact analysis, including the effects of bulkheads and of yielding supports. The main errors in this solution would be those caused by the finite length of bays.

CONCLUSION

The art of stress-analyzing shell structures is of recent origin, and any methods of analysis proposed must go through a process of trial and development.

Development of the method of shear-deformation analysis is desirable in several directions; e. g., exact

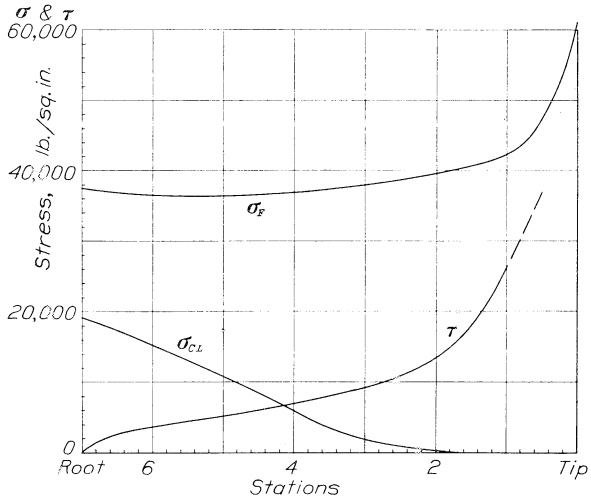

FIGURE 20.—Stresses in beam B with A_L uniformly distributed along chord.

solutions should be found to replace the constant-stress solution and methods should be devised to calculate the influence of bulkheads.

Rough approximate calculations on bulkhead effect can be made by assuming that all the longitudinals are relocated at the center line of the beam. For beams with a single longitudinal, the effect of bulkheads can be calculated. A series of systematic comparisons between the extended solution of Younger and Case 3 (a) of appendix B indicates that for a certain range the single-longitudinal assumption may yield acceptable approximations when used in conjunction with suitable correction factors. The comparisons are not given, however, because they might be misleading in view of the shear fault of Younger's solution. Calculations made thus far indicate that in practical cases the effect of the bulkheads is very small.

It should be emphasized that analyzing shell structures is an art rather than a science. The arithmetic of analyzing highly redundant structures can be reduced to manageable proportions only by making assumptions that will be valid only within a certain range. This fact leads to the unfortunate, but inevitable, conclusion that the analysis of such structures cannot be made entirely by handbook and formula but must be guided by engineering judgment.

LANGLEY MEMORIAL AERONAUTICAL LABORATORY,
NATIONAL ADVISORY COMMITTEE FOR AERONAUTICS,
LANGLEY FIELD, VA., *June 3, 1937.*

APPENDIX A

LIST OF SYMBOLS

A, cross-sectional area (sq. in.).
E, Young's modulus (lb. per sq. in.).
F, internal force (lb.).
G, shear modulus (lb. per sq. in.).
K, constant.
L, length of panel or beam (in.).
M, bending moment (in.-lb.).
P, external load (lb.).
S, shear force (lb.).
b, spacing of stringers (in.). (See figs. 3 and 4.)
b, half width of beam (in.). (See fig. 8.)
c, camber of cover (in.).
h, depth of beam (in.).
t, thickness of cover sheet (in.).
u, displacement of point (in.). (See fig. 4.)
w, running load (lb. per in.).
γ, shear strain.
σ, direct (normal) stress (lb. per sq. in.).
τ, shear stress (lb. per sq. in.).

Subscripts have the following significance:

A, loaded stringer A shown in figures 1, 2, 21, and 22.
B, unloaded stringer B shown in figures 1, 2, 21, and 22.
C, cover sheet.
F, flange of beam.
L, longitudinal of beam.
W, shear web.
a, applied shears and bending moments.
e, effective.
0, root section.
c, compression.
t, tension.
int, internal.
corr, corrected.
S, static equilibrium.
E, elastic equilibrium.
CL, center line.

APPENDIX B

SOLUTIONS OF DIFFERENTIAL EQUATIONS FOR SYMMETRICAL STRUCTURES OF CONSTANT CROSS SECTION

SIGN CONVENTIONS

Forces and stresses in stringers are positive when tensile. Shear forces and stresses in the sheet are positive when caused by positive stresses and strains in the loaded stringer A in the case of axially loaded panels or in the flange F in the case of beams.

CASE 1—THREE-STRINGER PANEL ON RIGID FOUNDATION WITH AXIAL LOAD

The two possible cases shown in figures 21(a) and 21(b) can be mathematically treated by taking one-half the panel, as shown in figure 21(c), which also

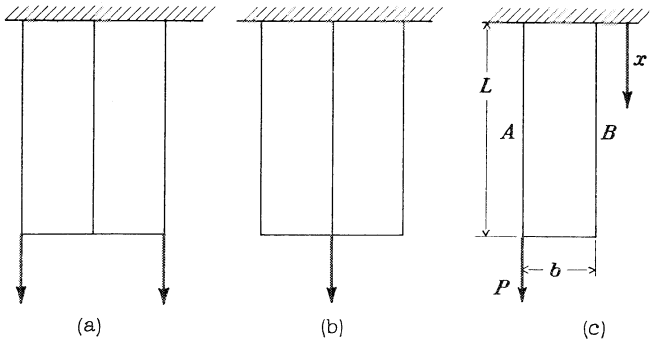

FIGURE 21.—Axially loaded panels.

gives the notation to be used. The derivation of the fundamental equations is given in the main body of this paper. Slightly modified for the purpose of deriving the basic differential equation, these equations are

$$\sigma_A' = \frac{\tau t}{A_A} \text{ and } \sigma_B' = -\frac{\tau t}{A_B} \tag{B-1}$$

$$\tau' = \frac{G_e}{Eb}(\sigma_A - \sigma_B) \tag{B-2}$$

where the primes denote differentiation with respect to x.

Differentiating equation (B–2) again and substituting into the result from equation (B–1),

$$\tau'' - \tau\frac{G_e t}{Eb}\left(\frac{1}{A_A}+\frac{1}{A_B}\right) = 0 \tag{B-3}$$

The boundary conditions are

$$\left.\begin{aligned} &\text{at} && x=0\ ,\ \tau=0 \\ &\text{at} && x=L\ ,\ \sigma_A=\frac{P}{A_A} \text{ and } \sigma_B=0 \end{aligned}\right\} \tag{B-4}$$

The result is

$$\left.\begin{aligned} \tau &= \frac{P}{A_A}\frac{G_e}{EbK}\frac{\sinh Kx}{\cosh KL} \\ \sigma_B &= \frac{P}{(A_A+A_B)}\left(1-\frac{\cosh Kx}{\cosh KL}\right) \\ \sigma_A &= \frac{P}{A_A}-\frac{A_B}{A_A}\sigma_B \end{aligned}\right\} \tag{B-5}$$

where

$$K^2 = \frac{G_e t}{Eb}\left(\frac{1}{A_A}+\frac{1}{A_B}\right) \tag{B-6}$$

In reference 2 the formula

$$f_b = \frac{2P}{A_T}\left[\frac{\cosh px - \tanh pL \sinh px}{4}+1\right]$$

where

$$p^2 = \frac{25}{2}\frac{G_e t}{A_T h E}$$

is given for the special case where the area of the edge stiffener is twice the area of the central stiffener. Taking account of the differences in notation and coordinate systems used, this result agrees with the general formula given under (B–5).

It should be noted that the final formulas (B–5) become invalid when either t or G_e approaches zero because in these cases the equation (B–3) becomes invalid. The solution for such cases is obtained by using the fundamental equations (B–1) and (B–2) directly.

An analogous procedure must be used for Cases 2 and 3.

CASE 2—THREE-STRINGER PANEL STRAINED BY MOTION OF SUPPORTS

The differential equation for the case of figure 22 is

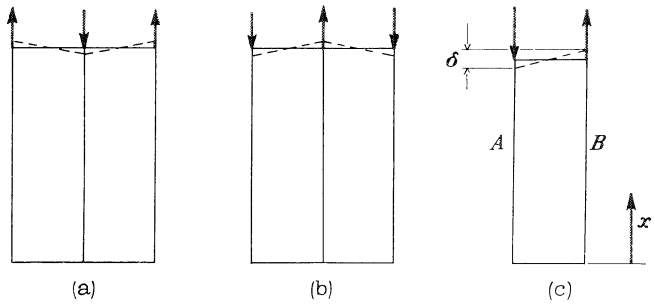

FIGURE 22.—Panels strained by motion of supports.

the same as for Case 1. The boundary conditions are now:

$$\left.\begin{aligned} &\text{at} && x=0\ ,\ \sigma_A=0 \text{ and } \sigma_B=0 \\ &\text{at} && x=L\ ,\ \tau=\frac{\delta}{b}G_e=\tau_0 \end{aligned}\right\} \tag{B-7}$$

The result is

$$\left.\begin{aligned} \tau &= \tau_0\frac{\cosh Kx}{\cosh KL} \\ \sigma_A &= -\tau_0\frac{t}{KA_A}\frac{\sinh Kx}{\cosh KL} \\ \sigma_B &= \tau_0\frac{t}{KA_B}\frac{\sinh Kx}{\cosh KL} \end{aligned}\right\} \tag{B-8}$$

where K has the same meaning as in (B–6).

CASE 3—CANTILEVER BEAM WITH ONE STRINGER

(*a*) Uniform depth, concentrated load at tip.
(*b*) Depth decreasing lineally to zero, uniformly distributed load.

Figure 8 shows the notation used for both cases. (Note that the x origin is at the tip.) The fundamental equations are for Case 3 (*a*)

$$\left.\begin{aligned} \sigma_F' A_F &= \frac{P}{h} - \tau t \\ \sigma_L' A_L &= \tau t \\ \tau' &= -\frac{G_e}{Eb}(\sigma_F - \sigma_L) \end{aligned}\right\} \quad \text{(B–9)}$$

which gives the differential equation

$$\tau'' - \tau \frac{G_e t}{Eb}\left(\frac{1}{A_F}+\frac{1}{A_L}\right) + \frac{PG_e}{A_F Ebh} = 0 \quad \text{(B–10)}$$

The boundary conditions are

$$\left.\begin{aligned} &\text{at} \quad x=0,\ \sigma_F=0, \text{ and } \sigma_L=0 \\ &\text{at} \quad x=L,\ \tau=0 \end{aligned}\right\} \quad \text{(B–11)}$$

The result is

$$\left.\begin{aligned} \tau &= \frac{P}{th\left(1+\frac{A_F}{A_L}\right)}\left(1-\frac{\cosh Kx}{\cosh KL}\right) \\ \sigma_L &= \frac{P}{h(A_L+A_F)}\left(x-\frac{\sinh Kx}{K\cosh KL}\right) \\ \sigma_F &= \frac{1}{A_F}\left(\frac{M_x}{h_x}-\sigma_L A_L\right) \end{aligned}\right\} \quad \text{(B–12)}$$

where K has again the same meaning as in (B–6) with A_F and A_L substituted for A_A and A_B.

In Case 3 (*b*), $wL/2$ is substituted for P; h in this case is the depth at the root.

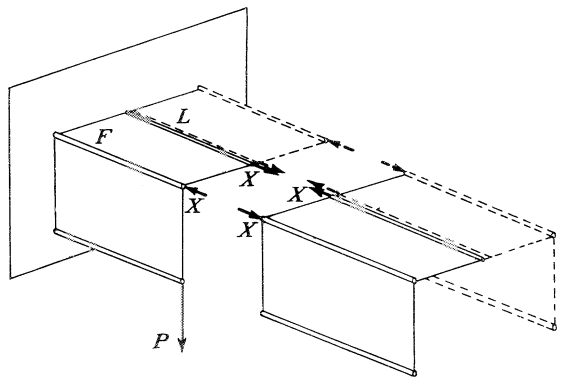

FIGURE 23.—Cantilever beam with concentrated load not at tip.

The case of a beam loaded by a concentrated load not at the tip is a simple problem in indeterminate structures. The beam is cut just outboard of the load (fig. 23) and the stresses in the cantilever part are calculated (Case 3 (*a*)). From these stressss, the distortion of the beam section at the cut; i. e., the relative displacement of the tips of the flange F and the longitudinal L, can be calculated. A system of forces X is then applied to equalize the distortion of the cantilever tip and of the inboard end of the "overhang," utilizing the formulas of Case 2.

CASE 4—CANTILEVER BEAM WITH ORTHOTROPIC COVER PLATE

Younger's solution for a beam of constant section.—The beam and the coordinate system used are shown in figure 17. *It should be noted that the x direction is opposite to that used in Cases 3 and 4.*

Under the assumptions that the transverse stresses and strains are negligible (Poisson's ratio equal to zero), and that G_e is independent of E, the differential equation of the cover is

$$\frac{\partial^2 u}{\partial y^2}+\frac{E}{G_e}\frac{\partial^2 u}{\partial x^2}=0 \quad \text{(B–13)}$$

where u is the displacement of any point on the cover in the x direction.

The boundary conditions are

$$\left.\begin{aligned} &\text{at} \quad x=0, \quad u=0 \text{ and } \frac{\partial u}{\partial y}=0 \\ &\qquad x=L, \frac{\partial u}{\partial x}=0 \\ &\qquad y=0, \frac{\partial u}{\partial y}=0 \end{aligned}\right\} \quad \text{(B–14)}$$

This equation was established by Younger (reference 4, pp. 36–47). For the solution he assumed that the external bending moment (on the whole beam) is given by

$$M=M_0 \cos\frac{\pi x}{2L} \quad \text{(B–15)}$$

and obtained for the longitudinal stress in the cover

$$\left.\begin{aligned} \sigma &= \frac{M_0 \cosh\frac{\pi y}{2KL}\cos\frac{\pi x}{2L}}{2h\left(A_F\cosh\frac{\pi b}{2KL}+\frac{A_L}{b}\frac{2KL}{\pi}\sinh\frac{\pi b}{2KL}\right)} \\ \text{and for the shear stress} \\ \tau &= \frac{M_0 G}{hE}\frac{\sinh\frac{\pi y}{2KL}\sin\frac{\pi x}{2L}}{2KA_F\cosh\frac{\pi b}{2KL}+\frac{4K^2tL}{\pi}\sinh\frac{\pi b}{2KL}} \end{aligned}\right\} \quad \text{(B–16)}$$

where K is defined by

$$K^2=\frac{G_e}{E} \quad \text{(B–17)}$$

Extension of Younger's solution.—Younger's solution can be somewhat extended. The external bending moment can be represented by a superposition of several terms:

$$M=M_1\cos\frac{\pi x}{2L}+M_3\cos\frac{3\pi x}{2L}+M_5\cos\frac{5\pi x}{2L} + \ldots + M_m\cos\frac{m\pi x}{2L} \quad \text{(B–18)}$$

where the m's are odd integers.

The values $M_1 \ldots M_m$ are chosen so that the sum of the terms equals the given external bending moment at m points other than the tip, where it is assumed that $M=0$. In order to make comparisons with Case 3, the bending moment caused by a tip load was expressed by

$$M=PL\left(0.821\cos\frac{\pi x}{2L}+0.101\cos\frac{3\pi x}{2L}+0.045\cos\frac{5\pi x}{2L}+0.033\cos\frac{7\pi x}{2L}\right) \quad \text{(B–19)}$$

The stresses corresponding to the mth term are given by

$$\left.\begin{aligned}\sigma_m&=\frac{M_m\cosh\frac{m\pi y}{2KL}\cos\frac{m\pi x}{2L}}{2h\left(A_F\cosh\frac{m\pi b}{2KL}+\frac{A_L}{b}\frac{2KL}{m\pi}\sinh\frac{m\pi b}{2KL}\right)}\\ \tau_m&=\frac{M_m}{h}\frac{G_e}{E}\frac{\sinh\frac{m\pi y}{2KL}\sin\frac{m\pi x}{2L}}{\left(2KA_F\cosh\frac{m\pi b}{2KL}+\frac{A_L 4K^2L}{bm\pi}\sinh\frac{m\pi b}{2KL}\right)}\end{aligned}\right\} \text{(B–16a)}$$

The assumptions of Poisson's ratio being zero and G being independent of E are, strictly speaking, incompatible. The physical picture conforming to these assumptions is not a plate but a system of stringers carrying only longitudinal stresses tied together by a sheet carrying only shear stresses. This picture is realized very nearly in practice by a skin-stringer cover, the only difference being that the total cross-sectional area of the stringers is not necessarily equal to the area of the sheet, as in the case of the plain cover sheet. All the equations written for the plain cover sheet apply, therefore, to the skin-stringer cover if only (B–17) is replaced by

$$K^2=R\frac{G_e}{E} \quad \text{(B–17a)}$$

where R is the ratio of sheet area to area of longitudinals.

Constant-stress solution.—The coordinate system is that shown in figure 17. Under the assumption that σ=constant for each longitudinal, the fundamental relation

$$\frac{d\tau}{dx}=\frac{G_e\Delta\sigma}{E\Delta y} \quad \text{(B–20)}$$

can be integrated once to give

$$\tau_x=\frac{\Delta\sigma}{E\Delta y}\int_0^x G_e dx=\frac{x\Delta\sigma}{E\Delta y}\overline{G}_x \quad \text{(B–21)}$$

where $\overline{G}_x$ is the shear stiffness averaged over the distance $x=0$ to $x=x$. Integrating again

$$S_C=\int_0^L \tau_x t dx=\int_0^L \frac{x}{E}\frac{\Delta\sigma}{\Delta y}\overline{G}_x t dx$$

In any given case this integration can be performed and the result is

$$S_C=K_2\frac{\Delta\sigma}{\Delta y} \quad \text{(B–22)}$$

where

$$K_2=\int_0^L \frac{x}{E}\overline{G}_x t dx$$

Now

$$S_C=\int_0^y \sigma\frac{A_L}{b}dy$$

(see fig. 24) or

$$\frac{dS_C}{dy}=\sigma\frac{A_L}{b} \quad \text{(B–23)}$$

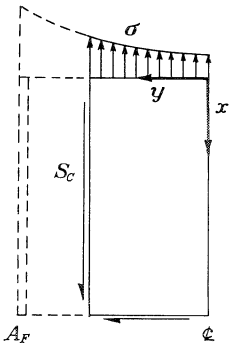

FIGURE 24.—Free-body diagram of cover plate.

Differentiating (B–22) and equating to (B–23)

$$\frac{d^2\sigma}{dy^2}-\sigma\frac{A_L}{bK_2}=0 \quad \text{(B–24)}$$

assuming that K_2 is independent of y.

The boundary conditions are

(1) at $y=0$, $\tau=0$ for any x. Therefore $\frac{d\sigma}{dy}=0$

(2) at any desired reference station R, the internal moment equals the external moment M_R.

The solution is

$$\sigma=\frac{M_R\cosh K_3 y}{h_R\left(A_F\cosh K_3 b+\frac{A_L}{bK_3}\sinh K_3 b\right)} \quad \text{(B–25)}$$

$$\tau=\sigma\frac{\overline{G}_x}{E}K_3 x\tanh K_3 y \quad \text{(B–26)}$$

where K_3 is defined by

$$K_3^2=\frac{A_L}{bK_2}=\frac{A_L}{b\int_0^L \frac{x}{E}\overline{G}_x t dx} \quad \text{(B–27)}$$

It may be noted that if G_e and t are not varied along the span, the constant K_3 is identical with the corresponding constant of Younger's solution except for a 10 percent difference in the numerical factor, namely, $\sqrt{2}$ against $\pi/2$.

APPENDIX C

ANALYSIS OF BEAM B

The dimensions and the loading of the beam are shown in table II.

ORDINARY BENDING THEORY

$$\sigma_F=\sigma_L=\sigma=\frac{M}{h(A_F+A_L)}=\frac{2{,}800{,}000}{24(1.875+1.875)}=$$
31,100 lb. per sq. in.

CONSTANT-STRESS SOLUTION

Since $\overline{G}_e$ is assumed constant along the span, $G_x=G_e$ and, from equation (7),

$$\tau_x=(\sigma_F-\sigma_L)\frac{xG_e}{Eb}$$

From equation (8)

$$S_C=\int_0^L(\sigma_F-\sigma_L)\frac{xG_e}{Eb}t_0\left(1-\frac{x}{L}\right)dx$$
$$=(\sigma_F-\sigma_L)\frac{G_et_0}{Eb}\int_0^L x\left(1-\frac{x}{L}\right)dx$$
$$=(\sigma_F-\sigma_L)\frac{0.2\times0.040}{24}\int_0^{280}x\left(1-\frac{x}{280}\right)dx$$
$$=4.35(\sigma_F-\sigma_L)$$
$$K_1=4.35$$

From equation (10a)

$$\sigma_L=\frac{2{,}800{,}000\times4.35}{24[1.875\times1.875+4.35(1.875+1.875)]}$$
$=25{,}550$ lb. per sq. in.

From equation (10b)

$$\sigma_F=\frac{2{,}800{,}000(1.875+4.35)}{24[1.875\times1.875+4.35(1.875+1.875)]}$$
$=36{,}500$ lb. per sq. in.

Substituting in equation (7) for the shear stress at the tip

$$\tau_{max}=(36{,}500-25{,}550)\frac{280\times0.2}{24}=25{,}560 \text{ lb. per sq. in.}$$

The calculation of the shear correction is shown in table III.

TRIAL-AND-ERROR SOLUTION

Take $\Delta x=40$ in.

$$\frac{S_W\Delta x}{h}=\frac{wxL\Delta x}{2h_0x}=\frac{wL}{2h_0}\Delta x=\frac{71.4\times280\times40}{2\times24}=16{,}670 \text{ lb.}$$

$$\Delta F_F=16{,}670-\Delta S_C$$

$$\Delta\tau=\frac{G_e\Delta x}{Eb}(\sigma_F-\sigma_L)=\frac{0.2\times40}{24}(\sigma_F-\sigma_L)=0.333(\sigma_F-\sigma_L)$$

A typical cycle of the calculation is shown in table IV.

REFERENCES

1. Younger, John E.: Miscellaneous Collected Airplane Structural Design Data, Formulas, and Methods. A. C. I. C. No. 644, Matériel Division, Army Air Corps, 1930.
2. White, Roland J., and Antz, Hans M.: Tests on the Stress Distribution in Reinforced Panels. Jour. Aero. Sci., vol. 3, no. 6, April 1936, pp. 209–212.
3. Lovett, B. B. C., and Rodee, W. F.: Transfer of Stress from Main Beams to Intermediate Stiffeners in Metal Sheet Covered Box Beams. Jour. Aero. Sci., vol. 3, no. 12, Oct. 1936, pp. 426–430.
4. Younger, John E.: Metal Wing Construction, Part II—Mathematical Investigations. A. C. T. R. ser. no. 3288, Matériel Division, Army Air Corps, 1930.

TABLE I.—ANALYSIS OF TENSION PANEL WITH SHEAR DEFORMATION

$A_A = 0.403$
$A_B = 0.220$
$t = 0.016$
$b = 4.60$

$L = 36$
$\Delta x = 6$
$F_A = 2,400 - \Sigma \Delta S_C$
$\sigma_A = \frac{F_A}{A_A} = \frac{F_A}{0.403}$

$F_B = \Sigma \Delta S_C$
$\sigma_B = \frac{F_B}{A_B} = \frac{F_B}{0.220}$
$G_e/E = 0.4$

$\Delta \tau = \frac{G_e \Delta x}{Eb}(\sigma_A - \sigma_B) = 0.522\ (\sigma_A - \sigma_B)$
$\tau = \Sigma \Delta \tau$
$\Delta S_C = \tau t \Delta x = 0.096\ \tau$

Station	By trial-and-error method									By formula [1]		
	ΔS_C (lb.)	F_A (lb.)	σ_A (lb./sq. in.)	F_B (lb.)	σ_B (lb./sq. in.)	$\sigma_A - \sigma_B$ (lb./sq. in.)	$\Delta \tau$ (lb./sq. in.)	τ (lb./sq. in.)	ΔS_C (lb.)	σ_A (lb./sq. in.)	σ_B (lb./sq. in.)	τ (lb./sq. in.)
0		2,400	5,960	0	0					5,960	0	5,230
	376							3,887	373			
1		2,024	5,020	376	1,708	3,312	1,730			5,022	1,717	2,885
	210							2,157	214			
2		1,814	4,500	586	2,662	1,838	960			4,502	2,670	1,584
	112							1,197	115			
3		1,702	4,224	698	3,170	1,054	550			4,220	3,186	856
	60							647	62			
4		1,642	4,075	758	3,444	631	329			4,070	3,461	442
	29							318	30			
5		1,613	4,005	787	3,575	430	224			3,996	3,595	187
	9							94	9			
6		1,604	3,980	796	3,618	362	189			3,968	3,630	0

[1] Appendix B, Case 1.

TABLE II.—CHARACTERISTICS OF BEAMS

The beams are assumed to be half beams as shown in fig. 8 (a).
All beams:

$h = 24$ in. at root.
$h = 0$ at tip.
$G_e/E = 0.2$.

$b = 24$ in.
$L = 280$ in.
$W = 71.4$ lb./in.

Beam	$A_F = A_L$ (sq. in.)		t (in.)		c
	Root	Tip	Root	Tip	
A	1.875	1.875	0.040	0.040	0.
B	1.875	0	.040	.000	0.
C	1.880	.470	.040	.010	0.

TABLE III.—CALCULATION OF SHEAR-FAULT CORRECTION FOR BEAM B

$\Delta x = 40$
$F_F = \sigma_F A_F = 36,500 A_F$
$\Delta S_{CS} = S_W \frac{\Delta x}{h} - \Delta F$

$\tau = 25,560 \frac{x}{L}$
$\Delta S_{CE} = \tau t \Delta x$
$\Delta S_C' = \Delta S_{CS} - \Delta S_{CE}$

$\sigma_F' = 0.5 \frac{S_C'}{A_F}$
$\sigma_L' = -0.5 \frac{S_C'}{A_L}$
$\sigma_{F_{corr}} = 36,500 + \sigma_F'$

$\sigma_{L_{corr}} = 25,550 + \sigma_L'$
$\tau' = 0.5 \frac{\Delta S_C'}{t \Delta x}$
$\tau_{corr} = \tau + \tau'$

Station	x from root (in.)	$A_F = A_L$ (sq. in.)	h (in.)	t (in.)	$S_W \frac{\Delta x}{h}$	F_F (lb.)	ΔF (lb.)	ΔS_{CS} (lb.)	τ (lb./sq. in.)	ΔS_{CE} (lb.)	$\Delta S_C'$ (lb.)	S_C' (lb.)	σ_F' (lb./sq. in.)	σ_L' (lb./sq. in.)	$\sigma_{F_{corr}}$ (lb./sq. in.)	$\sigma_{L_{corr}}$ (lb./sq. in.)	τ' (lb./sq. in.)	τ_{corr} (lb./sq. in.)
0																		
	260	0.134	1.71	0.00286	16,660		9,800	6,860	23,740	2,720	4,140						18,100	41,840
1		.268				9,800						4,140	7,720	−7,720	44,220	17,840		
	220	.402	5.14	.00857	16,660		9,800	6,860	20,080	6,880	−20						−30	20,050
2		.536				19,600						4,120	3,840	−3,840	40,340	21,720		
	180	.669	5.86	.0143	16,660		9,800	6,860	16,440	9,400	−2,540						−2,220	14,220
3		.804				29,400						1,580	986	−980	37,480	24,580		
	140	.937	12.00	.0200	16,660		9,800	6,860	12,780	10,220	−3,360						−2,100	10,680
4		1.072				39,200						−1,780	−830	830	35,670	26,390		
	100	1.205	15.42	.0257	16,660		9,800	6,860	9,130	9,400	−2,540						−1,230	7,900
5		1.340				49,000						−4,320	−1,610	1,610	34,890	27,170		
	60	1.473	18.87	.0314	16,660		9,800	6,860	5,480	6,880	−20						−10	5,470
6		1.608				58,800						−4,340	−1,350	1,350	35,150	26,910		
	20	1.740	22.28	.0371	16,660		9,800	6,860	1,826	2,710	4,150						1,400	3,226
7		1.875				68,600						−190	−50	50	36,450	25,610		

TABLE IV.—TRIAL-AND-ERROR SOLUTION FOR BEAM B

Station	x from root (in.)	$A_F = A_L$ (sq. in.)	$t \Delta x$	ΔS_C (lb.)	F_L (lb.)	σ_L (lb./sq. in.)	ΔF_F (lb.)	F_F (lb.)	σ_F (lb./sq. in.)	$\sigma_F - \sigma_L$ (lb./sq. in.)	$\Delta \tau$ (lb./sq. in.)	τ (lb./sq. in.)	ΔS_C (lb.)
0	280	0			0	0		0	0	0			
	260		0.1142	3,730			12,940					32,896	3,755
1	240	.268			3,730	13,920		12,940	48,280	34,360	11,453		
	220		.3426	7,440			9,230					21,443	7,340
2	200	.536			11,170	21,740		22,170	41,400	19,660	6,553		
	180		.571	8,680			7,990					14,890	8,500
3	160	.804			19,850	24,700		30,160	37,500	12,800	4,267		
	140		.799	8,670			8,000					10,623	8,490
4	120	1.072			28,520	26,620		38,160	35,600	8,980	2,993		
	100		1.028	8,070			8,600					7,630	7,840
5	80	1.340			36,590	27,300		46,760	34,880	7,580	2,527		
	60		1.255	6,360			10,310					5,103	6,400
6	40	1.608			42,950	26,700		57,070	35,470	8,770	2,923		
	20		1.485	3,130			13,540					2,180	3,240
7	0	1.875			46,080	24,560		70,610	37,640	13,080	4,360		

U. S. GOVERNMENT PRINTING OFFICE: 1937

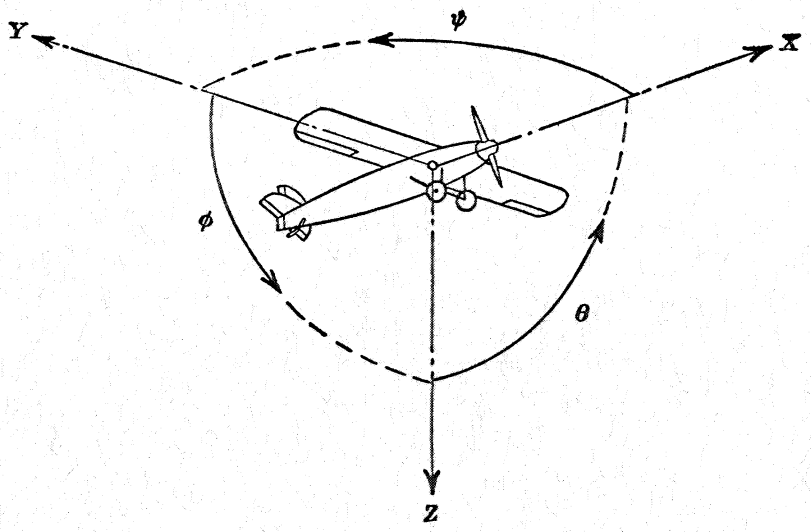

Positive directions of axes and angles (forces and moments) are shown by arrows

Axis		Force (parallel to axis) symbol	Moment about axis			Angle		Velocities	
Designation	Symbol		Designation	Symbol	Positive direction	Designation	Symbol	Linear (component along axis)	Angular
Longitudinal	X	X	Rolling	L	$Y \longrightarrow Z$	Roll	ϕ	u	p
Lateral	Y	Y	Pitching	M	$Z \longrightarrow X$	Pitch	θ	v	q
Normal	Z	Z	Yawing	N	$X \longrightarrow Y$	Yaw	ψ	w	r

Absolute coefficients of moment

$C_l = \frac{L}{qbS}$ (rolling) $\quad C_m = \frac{M}{qcS}$ (pitching) $\quad C_n = \frac{N}{qbS}$ (yawing)

Angle of set of control surface (relative to neutral position), δ. (Indicate surface by proper subscript.)

4. PROPELLER SYMBOLS

D, Diameter

p, Geometric pitch

p/D, Pitch ratio

V', Inflow velocity

V_s, Slipstream velocity

T, Thrust, absolute coefficient $C_T = \frac{T}{\rho n^2 D^4}$

Q, Torque, absolute coefficient $C_Q = \frac{Q}{\rho n^2 D^5}$

P, Power, absolute coefficient $C_P = \frac{P}{\rho n^3 D^5}$

C_s, Speed-power coefficient $= \sqrt[5]{\frac{\rho V^5}{P n^2}}$

η, Efficiency

n, Revolutions per second, r.p.s.

Φ, Effective helix angle $= \tan^{-1}\left(\frac{V}{2\pi r n}\right)$

5. NUMERICAL RELATIONS

1 hp.=76.04 kg-m/s=550 ft-lb./sec.

1 metric horsepower=1.0132 hp.

1 m.p.h.=0.4470 m.p.s.

1 m.p.s.=2.2369 m.p.h.

1 lb.=0.4536 kg.

1 kg=2.2046 lb.

1 mi.=1,609.35 m=5,280 ft.

1 m=3.2808 ft.